Magnetization compensation and spin reorientation transition in ferrimagnetic $DyCo_5$: Multiscale modeling and element-specific measurements

Andreas Donges,[1] Sergii Khmelevskyi,[2] Andras Deak,[3,4] Radu-Marius Abrudan,[5] Detlef Schmitz,[5] Ilie Radu,[6] Florin Radu,[5] László Szunyogh,[3,4] and Ulrich Nowak[1]

[1]*Fachbereich Physik, Universität Konstanz, Universitätsstraße 10, 78457 Konstanz, Germany*

[2]*Center for Computational Materials Science, Institute for Applied Physics, Vienna University of Technology, Wiedner Hauptstrasse 8, A-1040 Vienna, Austria*

[3]*Department of Theoretical Physics, Budapest University of Technology and Economics, Budafoki út 8, H-1111 Budapest, Hungary*

[4]*MTA-BME Condensed Matter Research Group, Budapest University of Technology and Economics, Budafoki út 8, H-1111 Budapest, Hungary*

[5]*Helmholtz-Zentrum Berlin für Materialien und Energie, 12489 Berlin, Germany*

[6]*Max-Born Institute, Max-Born-Strasse 2A, 12489 Berlin, Germany*

(Received 13 April 2017; published 11 July 2017)

We use a multiscale approach linking *ab initio* calculations for the parametrization of an atomistic spin model with spin dynamics simulations based on the stochastic Landau-Lifshitz-Gilbert equation to investigate the thermal magnetic properties of the ferrimagnetic rare-earth transition-metal intermetallic $DyCo_5$. Our theoretical findings are compared to elemental resolved measurements on $DyCo_5$ thin films using the x-ray magnetic circular dichroism technique. With our model, we are able to accurately compute the complex temperature dependence of the magnetization. The simulations yield a Curie temperature of $T_C = 1030$ K and a compensation point of $T_{comp} = 164$ K, which is in a good agreement with our experimental result of $T_{comp} = 120$ K. The spin reorientation transition is a consequence of competing elemental magnetocrystalline anisotropies in connection with different degrees of thermal demagnetization in the Dy and Co sublattices. Experimentally, we find this spin reorientation in a region from $T_{SR1,2} = 320$ to 360 K, whereas in our simulations the Co anisotropy appears to be underestimated, shifting the spin reorientation to higher temperatures.

DOI: 10.1103/PhysRevB.96.024412

I. INTRODUCTION

Intermetallics of the RCo_5 type, where R stands for a rare earth (RE), represent a highly intriguing class of magnetic materials with a variety of extraordinary properties. Due to the strong exchange coupling of the Co spins, these materials exhibit a high Curie temperature, far above room temperature. Furthermore, these compounds are known to exhibit large magnetocrystalline anisotropy energies up to several meV/f.u. [1]. Thus, compounds of the light REs, such as Y, Ce, Pr, and Sm, with ferromagnetic coupling to the Co sublattice and an easy c axis, are ideal for permanent magnet applications since they combine the aforementioned properties with a high magnetic energy density and high coercivity [1–4]. On the other hand, when fabricated with the heavy REs between Gd and Tm, there is an antiferromagnetic coupling to the Co sublattice, yielding ferrimagnetism [1]. For Tb, Dy, and Er, there exists a compensation temperature where the magnetizations of the Co and RE sublattices fully cancel each other [5–7]. Such a compensation point is seen as a prerequisite for thermally induced magnetization switching, where the magnetization is toggled by a fs-laser pulse on a sub-ps time scale [8–11], making these compounds promising research objects in the field of ultrafast magnetism. Additionally, there is a spin reorientation transition (SRT) in the RCo_5 compounds for Pr, Nd, Tb, Dy, and Ho, where the magnetization rotates from either an *easy-basal plane* (EBP) or *easy cone* (EC) to an *easy c axis* (EA) [12,13].

In this work, we implement a multiscale model to investigate $DyCo_5$ as a representative of this material class, as it combines most of the fascinating properties mentioned above. Moreover, $DyCo_5$ has been proposed to serve as pinning layer for semivolatile ferrimagnetic spin valves [14] and as a storage medium for magnetic-heat-assisted memory devices [15]. Although some theoretical work based on first-principles calculations has already been done on the RCo_5 intermetallics [16–19], we present a model combining fully relativistic *ab initio* calculations with atomistic spin model simulations based on the stochastic Landau-Lifshitz-Gilbert (LLG) equation of motion. Such a model can give insights into material properties beyond the ground state and at finite temperatures—a crucial requirement, considering the complex temperature dependence of the magnetic phases of these compounds [5,12,13]. This is especially important when studying magnetization compensation and SRT because both effects are caused by the different temperature dependence of the elemental magnetizations and anisotropies in the RE and Co sublattices.

Furthermore, we compare our theoretical findings to element-specific x-ray magnetic circular dichroism (XMCD) measurements. This technique is capable of measuring the orbital and spin magnetic moments of both specimens individually. In addition, we are able to measure the element-resolved hysteresis of the material, which allows us to identify the magnetization compensation point, the SRT temperature, as

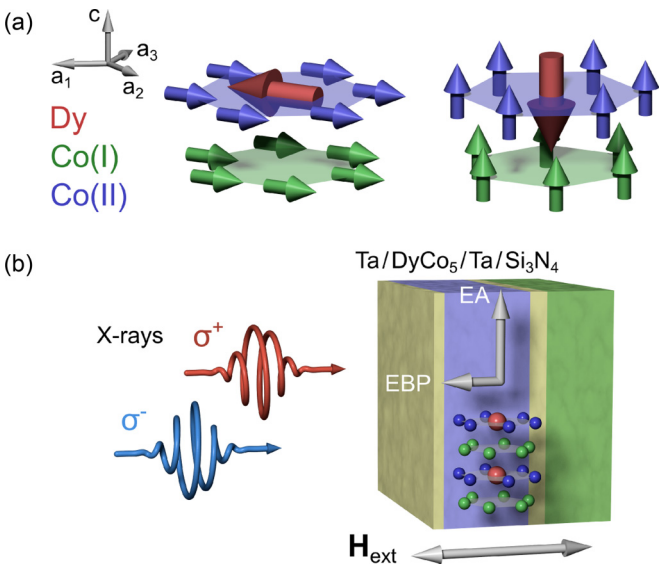

FIG. 1. (a) $CaCu_5$-type structure ($P6/mmm$) of ferrimagnetic $DyCo_5$, with EBP (left) and EA (right) magnetization, corresponding to the low- and high-temperature configurations, respectively. (b) Measurements geometry and sample composition. The c axis of the structure lies in the sample plane, which is the $[1\bar{1}00]$ plane; thus EBP (EA) magnetization is out of sample plane (in sample plane).

well as the element-specific anisotropy of the constituent elements.

II. MULTISCALE MODEL

A. *Ab initio* calculations

$DyCo_5$ has a hexagonal structure (space group $P6/mmm$) and three sublattices with the Wyckoff positions: Dy ($1a$ [0,0,0]), Co(I) ($3g$ [1/2,1/2,1/2]), and Co(II) ($2c$ [1/3,2/3,0]); see Fig. 1. In our calculations, we used the experimental lattice constants of $a = 4.929$ Å and $c = 3.986$ Å ($c/a = 0.809$) [20]. The self-consistent field (SCF) calculations were performed in terms of the Korringa-Kohn-Rostoker (KKR) method within the atomic sphere approximation (ASA) [21,22] and the local spin-density approximation (LSDA) with Perdew-Wang parametrization [23]. The ratio of the Wigner-Seitz radii of the Dy and Co atoms was chosen to be 1.25 and 3065 k points were sampled in the irreducible wedge of the Brillouin zone (IBZ). The nine $4f$ electrons of Dy were treated within the frozen-core approximation: seven f electrons with down spin and two f electrons with up spin, resulting in 5 μ_B spin moment and 5 μ_B orbital moment according to Hunds-rule coupling. The valence band was then modeled by using spd orbitals.

We performed SCF calculations for two different magnetic structures of $DyCo_5$, for the ferrimagnetic (FI) state, as depicted in Fig. 1, and the ferromagnetic (FM) state. In the FI state, we obtained the following valence-band spin moments: $\mu_{Dy} = -0.50\ \mu_B$, $\mu_{Co(I)} = -1.58\ \mu_B$, and $\mu_{Co(II)} = -1.50\ \mu_B$. Including the magnetic moment of 10 μ_B of the f electrons of Dy, in total this gives a magnetic moment of 1.76 μ_B for a formula unit. As expected, the FI state was lower in energy than the FM state, namely by 1.76 mRyd/atom.

Next we calculated the isotropic exchange interactions in the spirit of the magnetic force theorem [24]. Although we calculated the interactions within a distance of $2a$ of the atomic pairs, the nearest neighbor (NN) interactions turned out to play the dominating role. The Dy-Dy interactions are negligible, while the NN Co-Co interactions are strongly ferromagnetic with a value of about 1.1 mRyd. In particular, the Dy and the Co(II) moments are coupled antiferromagnetically with a NN interaction of -0.23 mRyd. Thus, the calculated Heisenberg interactions support the FI state as the magnetic ground state. Note that the Co moments are much stronger coupled to each other than to the Dy moments.

Furthermore, we used the coherent potential approximation (CPA) [21,22] to take into account a perturbed stoichiometry of $Dy_{1-x}Co_{5+x}$ with $x = 0.02$, following previous studies of RCo_5 intermetallics [25]. This perturbation neither affects the exchange interaction nor the induced magnetic moments significantly. The Co ions on the RE sites have a magnetic moment of $\mu_{Co(RE)} = -1.97\ \mu_B$ and couple ferromagnetically to the surrounding Co ions with a NN interaction of 0.53 mRyd.

The spin Hamiltonian for the normalized magnetic moments $\mathbf{S}_i = \boldsymbol{\mu}_i/\mu_i$ reads

$$\mathcal{H} = -\sum_{i,j} J_{ij}\mathbf{S}_i \cdot \mathbf{S}_j - \sum_i d^z_{2,i}\cos^2\vartheta_i - \sum_i d^6_{6,i}\sin^6\vartheta_i\cos(6\varphi_i) - \mathbf{B}\cdot\sum_i \mu_i\mathbf{S}_i, \quad (1)$$

where J_{ij} are the *ab initio* Heisenberg exchange constants, taking into account up to 11 shells per sublattice. $d^z_{2,i}$ is the uniaxial anisotropy constant, $d^6_{6,i}$ is the basal-plane anisotropy constant, and $\mathbf{B}$ is an external magnetic field. The basal-plane anisotropy was included in order to break the symmetry of the system in case the magnetization vector lies in the basal plane. For simplicity, the anisotropy energies were expressed in terms of the polar coordinates ϑ_i and φ_i of spin $\mathbf{S}_i$.

Due to the large $4f$ orbital moment, the magnetocrystalline anisotropy (MA) of Dy is known to be very high. Since the previously used scalar-relativistic frozen-core approximation cannot be used to calculate the MA energy, for this purpose we employed a relativistic LDA+U method employed within the KKR formalism [26,27]. Here we treated the $4f$ states of Dy within the LDA+U scheme by using the parameters $U = 7$ and $J = 0.7$ eV and calculated the MA energy in terms of the magnetic force theorem as a difference of the band energies corresponding to different orientations of the spin-quantization axis. The values of $d^z_{2,Dy} = -1.4$ mRyd (EBP anisotropy) and $d^6_{6,Dy} = 0.17$ mRyd were determined from our calculations. These values are in good agreement with previous experimental findings [25] and crystal-field calculations within the point-charge model [28,29], implying a direction for the ground-state magnetization as depicted in the upper left panel of Fig. 1. The calculated uniaxial anisotropy constants for the Co sublattices, $d^z_{2,Co(I)} = 0.0083$ and $d^z_{2,Co(II)} = 0.064$ mRyd, have the correct signs, i.e., EA anisotropy and, on average, are almost an order of magnitude larger than the uniaxial anisotropy of hcp Co (0.004 mRyd [30]). Nevertheless, their magnitude is strongly underestimated and insufficient to reach a reorientation transition below the Curie temperature. Thus

we needed to adjust these values to $d^z_{2,\mathrm{Co}} = 0.1$ mRyd per ion for each Co sublattice, which is compatible with calculations on other $R\mathrm{Co}_5$ compounds [16]. This discrepancy might be related to the strong dependence of the spin reorientation transition on the exact stoichiometry [31] and lattice constants [16]. As depicted in Fig. 1, the sample grows with its c axis in the sample plane; thus the EBP direction is out of plane and the EA direction is in plane. Finally, from our calculations, we obtained the orbital moment of the Co sublattices, which is 0.15 μ_B per atom.

B. Atomistic spin model

We use an atomistic spin model to compute the magnetic properties at elevated temperatures (see, e.g., Ref. [32]). This is done by numerical integration of the stochastic LLG equation,

$$\frac{\partial \mathbf{S}_i}{\partial t} = \frac{-\gamma_i}{(1+\alpha_i^2)\mu_i}\mathbf{S}_i \times (\mathbf{H}_i + \alpha_i \mathbf{S}_i \times \mathbf{H}_i), \qquad (2)$$

where γ_i is the gyromagnetic ratio and α_i is the Gilbert damping parameter, which couples the spin system to the electron and phonon heat baths. Since the focus of this paper is on the equilibrium properties, especially the spin reorientation transition, we can set $\alpha_i \sim 1$ in order to speed up the relaxation. The effective field $\mathbf{H}_i = -\partial\mathcal{H}/\partial\mathbf{S}_i + \boldsymbol{\zeta}_i(t)$ has a deterministic contribution from the spin Hamiltonian $\mathcal{H}$, as well as a temperature-dependent Langevin noise field $\boldsymbol{\zeta}_i$, which satisfies Gaussian white noise properties with

$$\langle \boldsymbol{\zeta}_i(t)\rangle = 0 \ \text{ and } \ \langle \boldsymbol{\zeta}_i(0)\boldsymbol{\zeta}_j^\dagger(t)\rangle = 2\alpha_i k_\mathrm{B} T \mu_i \delta_{ij}\delta(t)/\gamma_i. \qquad (3)$$

For the atomistic simulations, we used the perturbed stoichiometry of $\mathrm{Dy}_{0.98}\mathrm{Co}_{5.02}$ by randomly replacing 2% of the Dy spins on the lattice by Co spins, in the following called Co(RE). At $T = 0$, the Dy anisotropy per f.u. exceeds the one for the Co sublattices, and thus the ground state of the alloy is in the EBP direction. However, in such rare-earth transition-metal (RE-TM) alloys, the RE-RE exchange is much weaker than the TM-TM exchange. Therefore, with increasing temperature, the RE sublattice loses its magnetic order faster than those of the TM. This results not only in the magnetization compensation, but it also reduces the ratio of RE and TM anisotropy energies such that above a certain temperature, it is favorable for the system to align with the spins in the EA direction, i.e., along the Co easy axis, resulting in a SRT.

Since the anisotropy energies of the Dy and Co sublattices are approximately compensated close to the spin reorientation region, the energy difference between the in-plane and out-of-plane orientation is relatively small. Therefore the associated time scale of the rotation is slow and long simulation times are required, as well as large system sizes to reduce fluctuations of the magnetic vectors of the sublattices. We calculated the equilibrium magnetization on a lattice with 110 592 unit cells by initializing out of plane at $T = 0$ and increasing the temperature stepwise with a default simulation time equivalent to 50 ps, 100 ps close to the Curie temperature, and 200 ps close to spin reorientation transition. For each temperature step, the first half of the simulation time was used to equilibrate the magnetization and the latter half was used for the actual time average of the magnetization. In order to make sure that the system was properly equilibrated, we simulated every second data point close to the transition region with a stepwise decreasing temperature, starting with an in-plane magnetization. Although we treated the Co(I), Co(II), and Co(RE) sublattices separately for the calculations, the results below are shown for the weighted average of all Co spins, as they show very similar temperature dependences.

III. EXPERIMENTAL TECHNIQUES

DyCo_5 thin films (thickness 250 Å) have been grown by magnetron sputtering in an ultraclean Argon atmosphere of

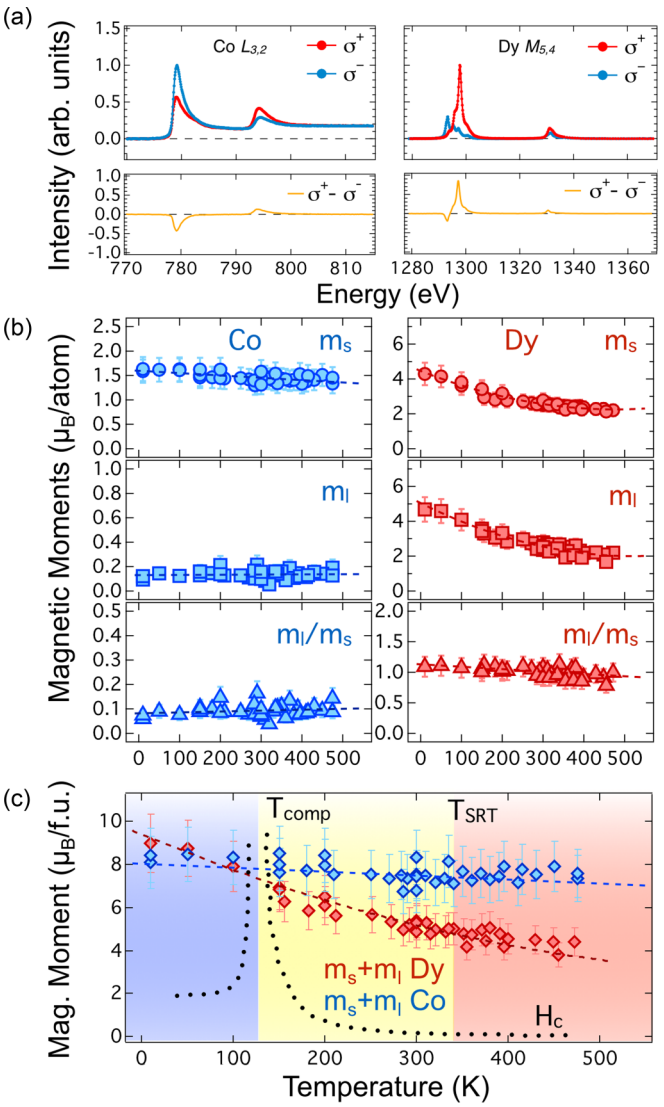

FIG. 2. (a) X-ray absorption spectroscopy data of DyCo_5 measured at Co and Dy edges for opposite magnetic fields (top red and blue curves) at room temperature. The resulting XMCD signal for Co and Dy is shown at the bottom. (b) Spin and orbital magnetic moments of Dy and Co vs temperature as deduced upon applying the magneto-optical sum rules [33–37]. The lowest frames show the orbital/spin moments ratios for both elements. The dashed lines are guides to the eye. (c) Stoichiometry-weighted (spin+orbital) magnetic moment of Dy and Co vs temperature; the curve's inflection point determines the magnetization compensation temperature region. For comparison, the coercive field is shown, with its divergence at the compensation point T_comp.

1.5×10^{-3} mbar with a base pressure of $<5 \times 10^{-9}$ mbar at a deposition temperature of 300 K. The stoichiometry of the ferrimagnetic alloy was controlled by varying the deposition rate of the separate elemental targets (Co and Dy) during the cosputtering process. Si_3N_4 membranes were used as substrates and thin Ta films were used as capping (30 Å) and buffer (50 Å) layers; see Fig. 1. Occurrence of both compensation at a temperature T_{comp} and the magnetic anisotropy reorientation within a temperature range $T_{SR1} < T_{SR2}$ is noticeable only in a reduced stoichiometry interval close to the stoichiometric $DyCo_5$ phase.

In order to measure the magnetic anisotropy changes and the variation of the elemental magnetic moments across the magnetization compensation and spin reorientation regions, we have employed the XMCD technique in the soft x-ray spectral range. The XMCD experiments were performed in transmission geometry at the Dy $M_{5,4}$ and Co $L_{3,2}$ absorption edges and covered the temperature range between 10 and 475 K. The XMCD spectra were recorded by detecting the transmitted signal for two opposite saturating magnetic fields or by flipping the helicity of the incoming circular x rays; in the latter case, the sample was kept magnetically saturated in a constant applied magnetic field. The element-specific hysteresis loops were recorded by setting the photon energy at the desired absorption edge (Dy M_5 or Co L_3) and measuring the transmitted intensity, while sweeping the magnetic field oriented perpendicular to the sample plane. The XMCD experiments at low temperatures and high magnetic fields were performed at the UE46-PGM1 beam line of HZB-BESSY II synchrotron, while the high-temperature experiments ($T >$ 200 K) were done using the ALICE diffractometer [38] installed at the PM3 [39] beam line of the same light source.

X-ray absorption spectroscopy (XAS) and its counterpart, the magnetic dichroism effect (XMCD), are routinely used to probe the ground-state **L** (orbital) and **S** (spin) magnetic moments using the well-established magneto-optical sum rules [33–37], thus being an ideal tool to study alloys with special magnetic structures. The sum rules relate the integrated XAS intensities measured at the resonant edges of the Co and Dy to the ground-state expectation value of spin and orbital magnetic moments (including the magnetic dipole operator) of the valence electrons [36,37].

The sum-rules equations for the Co and Dy orbital and spin moments were deduced from the general Eqs. (6) and (7) in Ref. [36], respectively. For Co ($2p \rightarrow 3d$ transition), the values of $c_{2p} = 1$ and $l_{3d} = 2$ were used for the orbital momentum quantum number of the core and the valence shell, as well as the value of $n_{3d} = 7.51$ for the $3d$ electron occupation number [33,40]. For Dy ($3d \rightarrow 4f$ transition), the values of $c_{3d} = 2$, $l_{4f} = 3$ and the electron occupation number of the $4f$ shells $n_{4f} = 9$ were used in the sum-rules calculations [41,42]. The magnetic dipole operator T_z is a measure of the field anisotropy for systems distorted by spin-orbit interaction or crystal-field effects [36]. For systems where the spin-orbit coupling is not large enough to prevent the edge ($L_{3,2}$ edges for $3d$ metals) overlap/intermixing, the T_z value is small and can be neglected. For $4f$ elements ($M_{5,4}$ edges), the strong spin-orbit coupling makes T_z rather large. Its value for Dy, evaluated analytically to be $-0.128\ \mu_B$ [36,42], was used in these calculations.

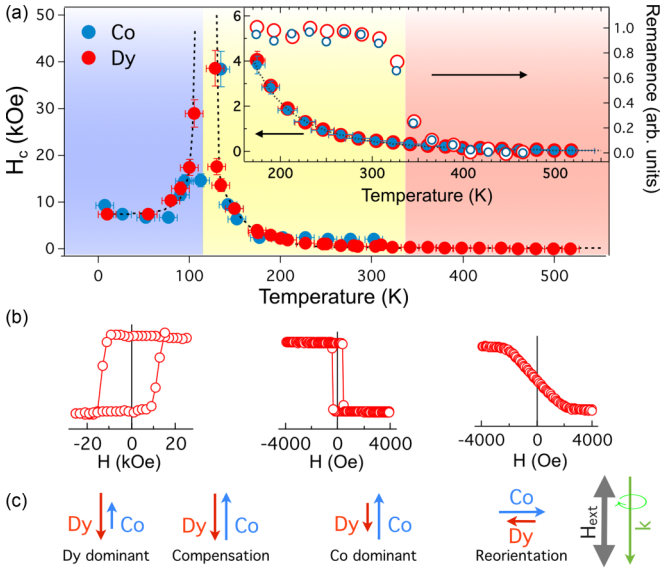

FIG. 3. (a) Temperature dependence of coercive field and out-of-plane remanent magnetization (upper panel inset) measured at Co L_3 and Dy M_5 edges. (b) Representative hysteresis loops (Dy M_5 edge) measured along the out-of-plane direction below and above the compensation temperature as well as above the spin reorientation temperature. (c) Schematic display of the Dy and Co magnetic moments' alignment as a function of temperature; incoming x-ray beam and the external applied magnetic field are depicted on the right-hand side.

IV. RESULTS AND DISCUSSION

Figure 2(a) presents selected results for XAS spectra of Co and Dy measured for opposite magnetic field orientations at the Co $L_{3,2}$ and Dy $M_{5,4}$ resonant edges, respectively. The shape and the sign of the XMCD signals at the Dy $M_{5,4}$ edges are consistent with data published on pure Dy samples [34] or previous data reported on RE-TM intermetallic compounds [43–45]. Moreover, the opposite XMCD polarity measured for Dy and Co demonstrates the ferrimagnetic character of the sample.

The obtained values of the spin and orbital magnetic moments as well as their ratio are plotted in Fig. 2(b). For Co, we obtained a spin magnetic moment of about 1.62 μ_B/atom at the lowest temperature that within the investigated temperature range, is decreasing only slightly upon increasing the temperature. The same behavior is seen for its orbital counterpart with a value of about 0.13 μ_B/atom. Such a slightly increased orbital moment is typical for magnets of the RCo_5 type [46,47] and agrees well with our *ab initio* value of 0.15 μ_B. The combined spin and orbital magnetic moment measured at the lowest temperature amounts to 1.75 μ_B/atom. For Dy, we have measured experimentally a spin moment of about 4.47 μ_B/atom and an orbital moment of 4.97 μ_B/atom by extrapolating the temperature dependence shown in Fig. 2(b) to 0 Kelvin. The combined spin and orbital magnetic moment of Dy measured experimentally as mentioned above amounts to 9.5 μ_B/atom. Note that these values of the magnetic moment agree closely with recent experimental measurements of Dy and Co moments of $DyCo_3$ and $DyCo_4$ compounds [44,45]. As compared to the temperature dependence of Co moments,

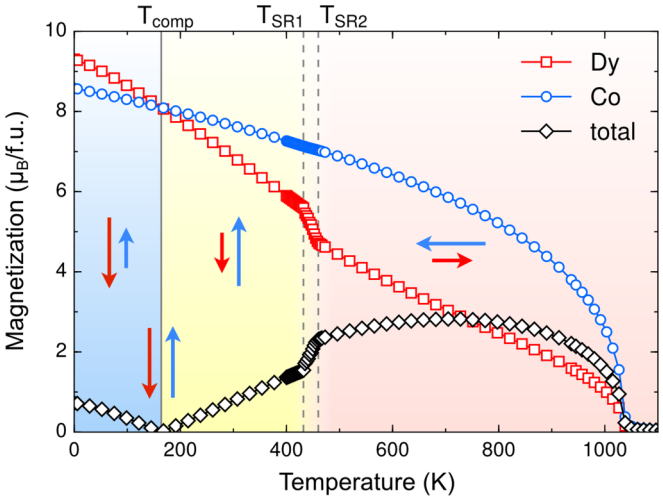

FIG. 4. Sublattice-resolved magnetization as a function of temperature from atomistic simulations. The solid vertical line shows the magnetization compensation point $T_{comp} = 164$ K. The SRT region is indicated by the dashed lines, with starting point $T_{SR1} = 432$ K and end point $T_{SR2} = 460$ K, clearly visible by the steep slope of the magnetization in this temperature range. A Curie temperature of 1030 K is found in the simulations, in reasonable agreement with previous experiments [5,25].

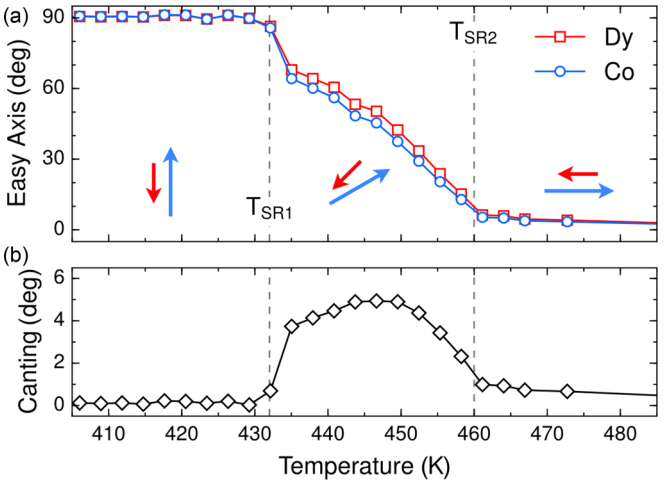

FIG. 5. (a) Simulation results for direction of the easy axis of $DyCo_5$ with respect to the c axis. With increasing temperature, the magnetization rotates from the EBP direction (90°) to the EA direction (0°/180°). (b) Within the reorientation region $T_{SR1} < T < T_{SR2}$, i.e., for the EC magnetization, the Dy and Co spins are no longer aligned perfectly antiparallel, but show a finite canting of up to 5°. Co orientation has been mirrored for better comparison.

the spin and orbital moments of Dy exhibit a much stronger dependence on temperature, which fits well with the theoretical simulations (see Fig. 4).

In the low-temperature range below compensation, Dy is the dominant magnetic sublattice that aligns parallel to the external magnetic field, as can be seen from the schema in Fig. 3(b) and the stoichiometry-weighted (spin+orbital) magnetic moments of Dy and Co in Fig. 3(c). Upon increasing the temperature, the different degrees of demagnetization of the Dy and Co sublattices lead to a full compensation of the magnetization. The experimental fingerprint of the magnetization compensation temperature is the divergence of the coercive field (due to zero net magnetization), which can be clearly seen at $T_{comp} = 120$ K for both elements in Fig. 3(a). This is further corroborated by the inflection region of the Dy and Co magnetization, as shown in Fig. 2(c). As expected, in the magnetization compensation region, the elemental magnetic moments are of equal magnitude and lead to a zero net magnetization due to their antiferromagnetic coupling. This value is in rather good agreement with the simulation data in Fig. 4, where the compensation point is at 164 K. The discrepancy between measured and simulated compensation point can be further reduced by increasing the Co(RE)/Dy ratio, resulting in a shift of T_{comp} of approximately -20 K per percentage point of Co(RE) substitution. The position of the compensation point moreover depends on the faster demagnetization of the Dy sublattice, which is associated with the weaker Dy exchange field. From the vicinity of measured and computed compensation point, we can thus conclude that the antiferromagnetic Dy-Co exchange couplings from our *ab initio* calculations have the correct strength, since the weak RE-RE couplings in the RCo_5 structure barely contribute to the overall RE exchange field.

Figure 5 shows the orientation of the equilibrium magnetization, defined as the angle between the magnetization vector and the c axis, for the Dy and Co spins, as a function of temperature from our atomistic simulations. The spin reorientation is found to start at a temperature of $T_{SR1} = 432$K, when the magnetization rotates from the out-of-plane or EBP to the EC direction. At $T_{SR2} = 460$K, the rotation is complete and the magnetization is now fully in plane, i.e., along the EA direction. This matches qualitatively with the experimental findings, but at different temperatures, which is linked to the underestimation of the Co anisotropy in our model. In Fig. 3, we show the temperature dependence of the coercive field and the normalized remanent magnetization that was measured for the $DyCo_5$ sample. Below $T_{SR1} = 320$ K, the hysteresis shows a square-loop shape with a high remanent magnetization characteristic of systems with high magnetocrystalline anisotropy. By further increasing the temperature, we can see that beyond $T_{SR2} = 360$ K, a hard axis hysteresis with no remanent magnetization was measured. This clearly shows a rotation of the magnetic anisotropy from out of plane to in plane, or from EBP to EA, respectively.

From our multiscale model, we can also see that in the EC phase in between T_{SR1} and T_{SR2}, the RE and the TM sublattices no longer align perfectly colinear, but have a finite canting which can reach up to 5°, shown in the lower panel of Fig. 5. Although this value is too small to be resolved experimentally, such a canting corresponds to an excitation of the antiferromagnetic exchange coupling of several hundred μeV/f.u. Indirect experimental evidence of such a noncollinear alignment can be found in the related RE-TM intermetallic $HoCo_3Ni_2$, where only a partial magnetization compensation was found, occurring in the EC phase between T_{SR1} and T_{SR2} [48].

The reorientation can also be observed in the absolute value of the magnetization, as displayed in Fig. 4. Below

T_{SR1} and above T_{SR2}, we find a basically constant slope of the Dy magnetization up to almost T_C. However, at the spin reorientation, the slope of the Dy magnetization is discontinuous, increasing by more than a factor of 3. This jump in the Dy demagnetization rate can be explained by the large anisotropy energy of the Dy spins that contributes significantly to their overall effective field. Thus the anisotropy field is not only responsible for the orientation of the magnetization with respect to the lattice, but also for the microscopic magnetic ordering. When the Dy spins are then forced into their hard axis, the effective field is reduced by the anisotropy field and the absolute value of its sublattice magnetization decreases. For the Co sublattice, on the other hand, the anisotropy energy per ion is two orders of magnitude smaller than the Heisenberg exchange, thus too small to have an effect on the microscopic magnetic ordering. These findings are consistent with previous neutron-diffraction [25] and magnetometry measurements [5,49] on bulk $DyCo_5$. The effect is not observed in our XMCD measurements in Fig. 2 due to the application of a saturating field in the out-of-plane direction, keeping the magnetic moments of Dy aligned along their easy axis even at temperatures above T_{SR2}. It should also be noted that the almost constant Co magnetization in Fig. 2 deviates from the simulation results in Fig. 4 due to the semiclassical nature of our model that does not follow Bloch's $T^{3/2}$ law [50]. As shown by Watson *et al.* [51], at low temperature, the classical model shows a linear demagnetization $\sim 0.36 \times T/T_C$ instead, and hence the magnetic ordering of the Co spins and the remanent magnetization above T_{comp} is slightly reduced in our simulations. Nevertheless, the temperature dependence of the total magnetic moments in Fig. 4 shows excellent agreement with earlier magnetometry measurements performed by Tsushima and Ohokoshi [5]. Finally, from our simulations, we obtain a Curie temperature of about 1030 K, which is close to the reported values between 925 and 970 K [5,13]. This suggests that the calculated ferromagnetic Co-Co exchange interactions have the correct magnitude.

Before concluding the paper, we would like to shortly discuss the potential of ferrimagnetic $DyCo_5$ for future time-resolved magnetization dynamics studies. As described here, $DyCo_5$ exhibits both a magnetization compensation temperature around 120 K and a SRT between 320 K and 360 K. Thus, by simply using an ultrashort laser-induced heating of the sample and choosing the proper steady-state sample temperature, one could photo drive and investigate three different dynamic spin phenomena on the very same sample: magnetization switching across the compensation temperature [8], laser-induced demagnetization [52], and the laser-induced spin reorientation transition [53]. Moreover, given the large differences in magnetic moments of Dy and Co and the large orbital magnetic moment on Dy, one could investigate how these quantities would affect the ultrafast element-specific dynamics (see, e.g., Ref. [54]) and the average magnetization response when the system goes through the magnetic phase transitions mentioned above.

In conclusion, we have shown that our multiscale model of *ab initio* calculations and atomistic spin dynamics simulations is capable to describe the complex magnetic properties of the RCo_5 intermetallics, beyond the molecular-field theory. We have shown that the SRT in this material class is caused by the different temperature dependence of the competing magnetocrystalline anisotropies of the RE and Co spins and can thus be understood as a statistical effect within a semiclassical framework. The calculated magnetization compensation point as well as the SRT are in good agreement with our element-specific measurements.

ACKNOWLEDGMENTS

This work was supported by the European Community's Seventh Framework Programme FP7/2007-2013 under Grant Agreement No. 281043, FEMTOSPIN. Furthermore, A. Donges and U.N. would like to acknowledge financial support by the *Center for Applied Photonics* at the University of Konstanz, while A. Deak and L.S. acknowledge the support by the Hungarian Scientific Research Fund (NKFIH) under Project No. K115575. I.R. acknowledges financial support from the German Federal Ministry of Education and Research (BMBF) through Project No. 05K16BCA. The authors thank Helmholtz-Zentrum Berlin for the allocation of synchrotron radiation beam time at BESSY II Berlin. The ALICE project was supported by the BMBF Contract No. 05K10PC2.

[1] K. Strnat, G. Hoffer, J. Olson, W. Ostertag, and J. J. Becker, J. Appl. Phys. **38**, 1001 (1967).

[2] J. Zhang, H. Gao, Y. Yan, X. Bai, F. Su, W. Wang, and X. Du, J. Magn. Magn. Mater. **324**, 3272 (2012).

[3] W. Wallace, T. Volkmann, and H. Hopkins, J. Solid State Chem. **3**, 510 (1971).

[4] P. Larson, I. I. Mazin, and D. A. Papaconstantopoulos, Phys. Rev. B **69**, 134408 (2004).

[5] T. Tsushima and M. Ohokoshi, J. Magn. Magn. Mater. **31-34**, Part 1, 197 (1983).

[6] R. Ballou, B. Gorges, R. Lemaire, H. Rakoto, and J. Ousset, Phys. B: Condens. Matter **155**, 266 (1989).

[7] Z. Drzazga and T. Mydlarz, Phys. Status Solidi **80**, 403 (1983).

[8] I. Radu, K. Vahaplar, C. Stamm, T. Kachel, N. Pontius, H. A. Dürr, T. A. Ostler, J. Barker, R. F. L. Evans, R. W. Chantrell, A. Tsukamoto, A. Itoh, A. Kirilyuk, T. Rasing, and A. V. Kimel, Nature (London) **472**, 205 (2011).

[9] T. A. Ostler, J. Barker, R. F. L. Evans, R. W. Chantrell, U. Atxitia, O. Chubykalo-Fesenko, S. E. Moussaoui, L. L. Guyader, E. Mengotti, L. J. Heyderman, F. Nolting, A. Tsukamoto, A. Itoh, D. Afanasiev, B. A. Ivanov, A. M. Kalashnikova, K. Vahaplar, J. Mentink, A. Kirilyuk, T. Rasing, and A. V. Kimel, Nat. Commun. **3**, 666 (2012).

[10] S. Wienholdt, D. Hinzke, K. Carva, P. M. Oppeneer, and U. Nowak, Phys. Rev. B **88**, 020406 (2013).

[11] L. Le Guyader, S. El Moussaoui, M. Buzzi, M. Savoini, A. Tsukamoto, A. Itoh, A. Kirilyuk, T. Rasing, F. Nolting, and A. V. Kimel, Phys. Rev. B **93**, 134402 (2016).
[12] T.-s. Zhao, H.-m. Jin, G.-h. Guo, X.-f. Han, and H. Chen, Phys. Rev. B **43**, 8593 (1991).
[13] A. Andreev and S. Zadvorkin, Phys. B: Condens. Matter **172**, 517 (1991).
[14] F. Radu, U.S. Patent No. 14/383,131 (1 Mar 2013).
[15] A. A. Ünal, S. Valencia, F. Radu, D. Marchenko, K. J. Merazzo, M. Vázquez, and J. Sánchez-Barriga, Phys. Rev. Appl. **5**, 064007 (2016).
[16] H. Pang, L. Qiao, and F. S. Li, Phys. Status Solidi **246**, 1345 (2009).
[17] G. I. Miletić and Ž. Blažina, J. Solid State Chem. **180**, 604 (2007).
[18] G. I. Miletić and Ž. Blažina, J. Magn. Magn. Mater. **321**, 3888 (2009).
[19] G. I. Miletić and Ž. Blažina, J. Magn. Magn. Mater. **321**, 2300 (2009).
[20] D. Banerjee, D. Bahadur, K. Suresh, and A. Nigam, Phys. B: Condens. Matter **378-380**, 1091 (2006).
[21] I. A. Abrikosov and H. L. Skriver, Phys. Rev. B **47**, 16532 (1993).
[22] A. Ruban and H. Skriver, Comput. Mater. Sci. **15**, 119 (1999).
[23] J. P. Perdew and Y. Wang, Phys. Rev. B **45**, 13244 (1992).
[24] A. Liechtenstein, M. Katsnelson, V. Antropov, and V. Gubanov, J. Magn. Magn. Mater. **67**, 65 (1987).
[25] V. V. Kelarev, V. V. Chuev, A. N. Pibogov, and S. K. Sidoeov, Phys. Status Solidi **79**, 57 (1983).
[26] H. Ebert, A. Perlov, and S. Mankovsky, Solid State Commun. **127**, 443 (2003).
[27] L. Oroszlány, A. Deák, E. Simon, S. Khmelevskyi, and L. Szunyogh, Phys. Rev. Lett. **115**, 096402 (2015).
[28] R. Radwański, J. Magn. Magn. Mater. **62**, 120 (1986).
[29] R. Radwański, J. Phys. F **17**, 267 (1987).
[30] D. Paige, B. Szpunar, and B. Tanner, J. Magn. Magn. Mater. **44**, 239 (1984).
[31] D. Banerjee, K. G. Suresh, and A. K. Nigam, J. Magn. Magn. Mater. **320**, 374 (2008).
[32] U. Nowak, Classical spin models, in *Handbook of Magnetism and Advanced Magnetic Materials*, edited by H. Kronmueller and S. Parkin (Wiley, New York, 2007).
[33] C. T. Chen, Y. U. Idzerda, H.-J. Lin, N. V. Smith, G. Meigs, E. Chaban, G. H. Ho, E. Pellegrin, and F. Sette, Phys. Rev. Lett. **75**, 152 (1995).
[34] J. Vogel, M. Sacchi, F. Sirotti, and G. Rossi, Appl. Surf. Sci. **65**, 170 (1993).
[35] Y. Teramura, A. Tanaka, and T. Jo, J. Phys. Soc. Jpn. **65**, 1053 (1996).
[36] P. Carra, B. T. Thole, M. Altarelli, and X. Wang, Phys. Rev. Lett. **70**, 694 (1993).
[37] B. T. Thole, P. Carra, F. Sette, and G. van der Laan, Phys. Rev. Lett. **68**, 1943 (1992).
[38] R. Abrudan, F. Brüssing, R. Salikhov, J. Meermann, I. Radu, H. Ryll, F. Radu, and H. Zabel, Rev. Sci. Instrum. **86**, 063902 (2015).
[39] T. Kachel, F. Eggenstein, and R. Follath, J. Synchrotron Rad. **22**, 1301 (2015).
[40] G. Schütz, E. Goering, and H. Stoll, in *Handbook of Magnetism and Advanced Magnetic Materials*, edited by H. Kronmueller and S. Parkin (Wiley, Chichester, UK, 2007), pp. 1311–1363.
[41] J. Dreiser, K. S. Pedersen, C. Piamonteze, S. Rusponi, Z. Salman, M. E. Ali, M. Schau-Magnussen, C. A. Thuesen, S. Piligkos, H. Weihe *et al.*, Chem Sci. **3**, 1024 (2012).
[42] Y. Teramura, A. Tanaka, B. Thole, and T. Jo, J. Phys. Soc. Jpn. **65**, 3056 (1996).
[43] F. Radu, R. Abrudan, I. Radu, D. Schmitz, and H. Zabel, Nat. Commun. **3**, 715 (2012).
[44] K. Chen, D. Lott, F. Radu, F. Choueikani, E. Otero, and P. Ohresser, Phys. Rev. B **91**, 024409 (2015).
[45] K. Chen, D. Lott, F. Radu, F. Choueikani, E. Otero, and P. Ohresser, Sci. Rep. **5**, 18377 (2015).
[46] A. Heidemann, D. Richter, and K. H. J. Buschow, Z. Phys. B Condens. Matter **22**, 367 (1975).
[47] J. Schweizer and F. Tasset, J. Phys. F **10**, 2799 (1980).
[48] Z. Drzazga, J. Magn. Magn. Mater. **25**, 11 (1981).
[49] M. Ohkoshi, H. Kobayashi, T. Katayama, M. Hirano, and T. Tsushima, Physica B+C **86**, 195 (1977).
[50] F. Bloch, Z. Phys. **61**, 206 (1930).
[51] R. E. Watson, M. Blume, and G. H. Vineyard, Phys. Rev. **181**, 811 (1969).
[52] R. Abrudan *et al.* (unpublished).
[53] A. Kimel, A. Kirilyuk, A. Tsvetkov, R. Pisarev, and T. Rasing, Nature (London) **429**, 850 (2004).
[54] I. Radu, C. Stamm, A. Eschenlohr, F. Radu, R. Abrudan, K. Vahaplar, T. Kachel, N. Pontius, R. Mitzner, K. Holldack *et al.*, SPIN **05**, 1550004 (2015).